Thin Solid Films 520 (2012) 1832–1836

Contents lists available at SciVerse ScienceDirect

Thin Solid Films

journal homepage: www.elsevier.com/locate/tsf

Control of ZnO thin film surface by ZnS passivation to enhance photoluminescence

Jeong-Yeon Hwang [a,b], Sung Youl Park [a], Jong-Ho Park [a], Jong-Nam Kim [a], Sang Man Koo [b,*], Chang Hyun Ko [a,**]

[a] Korea Institute of Energy Research, 102, Gajeong-ro, Yuseong-gu, Daejeon, 305-343, Republic of Korea
[b] Department of Chemical Engineering, Hanyang University, 17 Haengdang-dong, Sungdong-gu, Seoul 133-791, Republic of Korea

ARTICLE INFO

Article history:
Received 25 October 2010
Received in revised form 25 August 2011
Accepted 30 August 2011
Available online 6 September 2011

Keywords:
Atomic layer deposition
Zinc oxide
Zinc sulfide
Photoluminescence
Multi-layer

ABSTRACT

To enhance the optical property of zinc oxide (ZnO) thin film, zinc sulfide (ZnS) thin films were formed on the interfaces of ZnO thin film as a passivation and a substrate layer. ZnO and ZnS thin films were deposited by atomic layer deposition (ALD) using diethyl zinc, H_2O, and H_2S as precursors. Investigations by X-ray diffraction and transmission electron microscopy showed that ZnS/ZnO/ZnS multi-layer thin films with clear boundaries were achieved by ALD and that each film layer had its own polycrystalline phase. The intensity of the photoluminescence of the ZnO thin film was enhanced as the thickness of the ZnO thin film increased and as ZnS passivation was applied onto the ZnO thin film interfaces.

1. Introduction

As an important II–VI group compound semiconductor, ZnO has a wide band-gap energy of 3.37 eV with a high exciton binding energy of 60 meV. It is also thermally and chemically stable at high temperatures [1]. The unique optical and electronic properties of ZnO make it applicable in a wide range of applications such as, photonic devices [2], UV-emitting diodes [3], and transparent conducting electrodes for solar cells [4].

For these applications with high-quality thin films, various types of deposition methods have been reported, including metal organic chemical vapor deposition (MOCVD) [5], spray pyrolysis [6], pulsed laser deposition [7], RF or DC magnetron sputtering [8,9], and atomic layer deposition (ALD) [4,10]. Among these methods, ALD is a self-limiting thin-film growth method that involves alternating surface reactions between gas phase precursors and a solid surface. Thus, it has practical advantages for the growth of thin films with precise thickness control at the atomic scale, coverage of large areas, very good conformality, and reasonable uniformity even at low temperatures [10–12]. These characteristics of ALD have enabled the formation of thin films on various types of substrates, such as powders [13], nanoporous membranes [14,15], and high-aspect-ratio structures [16]. Another advantage is that multi-layer films can be grown with specific optical properties [17]. The typical photoluminescence spectra of ZnO are characterized by a sharp, UV band-edge emission and more broad and visible emission peaks. The different visible emissions of ZnO are primarily caused by crystal surface defects that form according to the experimental conditions of the ZnO thin film deposition process [18]. Improvement of the optical properties of ZnO prepared by ALD has been attempted by optimizing the thin film formation temperature [19,20], the annealing temperature with various gas environments after film formation [21], and by including hetero- and homo-buffers [22,23]. However, there is considerable room for improvement of the optical properties of ZnO thin film, particularly in how surface defects are controlled.

In this paper, ZnS thin films prepared by ALD are introduced as both a substrate layer and a passivation layer to enhance the photoluminescence of ZnO. X-ray diffraction patterns and cross-sectional TEM images reveal that a poly-crystalline, clearly distinguished ZnS/ZnO/ZnS multi-layer can be formed by ALD. The presence of the passivation layer is closely related to the photoluminescence intensity of the ZnO.

2. Experimental section

Before the ZnO deposition process, the particles and surface native oxide layer on a Si(100) wafer were removed by a SC-1 solution ($NH_4OH:H_2O_2:H_2O = 1:1:5$) and a diluted hydrofluoric (DHF) solution ($HF:H_2O = 1:10$). First, the Si(100) substrates were cleaned with diluted solution of detergent RBS-25 [Chemical Products R. Borghgraef S.A. (Belgium), RBS-25:H_2O (de-ionized water) = 1:10 (weight ratio)] for 10 min after which they were immediately

* Corresponding author. Tel.: +82 2 2220 0527; fax: +82 2 2281 4800.
** Corresponding author. Tel.: +82 42 860 3132; fax: +82 42 860 3134.
E-mail addresses: sangman@hanyang.ac.kr (S.M. Koo), chko@kier.re.kr (C.H. Ko).

0040-6090/$ – see front matter © 2011 Elsevier B.V. All rights reserved.
doi:10.1016/j.tsf.2011.08.108

washed. Second, the surface layer was etched with a SC-1 solution for approximately 10 min at 80–100 °C and then a HF solution for 1 min at 80–90 °C. After each process was conducted, the treated substrates were immediately washed with H_2O.

ZnO, ZnS, and Al_2O_3 thin films were deposited by the ALD method in a commercialized reaction system (MP-1000 from ASM-Genitech). Amorphous Al_2O_3 thin films with a thickness of approximately 17 nm were deposited using the precursors of $Al(CH_3)_3$ [tri-methyl aluminum (TMA)] (Sunwretech) and H_2O. The ZnO thin films were deposited using $Zn(C_2H_5)_2$ [diethyl zinc (DEZn)] (Sunwretech) and H_2O as precursors. For the ZnS thin film, DEZn and H_2S (Korea Noble Gas) were selected as the precursors. One cycle of the ALD deposition process consisted of 4 steps: 1) metal precursor feeding, 2) purging, 3) oxygen or sulfur precursor feeding, and 4) purging. The step times for each thin film are summarized in Table 1. Argon was used as a precursor carrier and for reactant purging. The substrate temperature was maintained at 300 °C. The reactor pressure during the process was maintained at 400 Pa. The film thickness was measured by the change in the light reflectivity using a ST2000DLXn (Korea Materials & Analysis Corporation). The X-ray diffraction (XRD) patterns of the ZnO thin films were obtained in the 2θ range from 20° to 80° at a grazing incidence of 0.6° using a diffractometer (Rigaku, DMAX-2500) with Cu Kα radiation at 40 kV and 126 mA. The XRD patterns were compared to the ICDD data for material identification. Cross-sectional images of the ZnO thin films were obtained using a Field Emission Transmission Electron Microscope (FE-TEM, Technai F30 S-Twin, installed at NNFC, with an operating voltage of 300 kV). Room-temperature photoluminescence (PL) measurements were obtained using a Spex 1400p spectrometer operating under excitation of 325 nm from a He–Cd laser with 1 mW of power as a light source.

3. Results and discussion

Fig. 1 shows the increase in the film thickness of Al_2O_3, ZnO, and ZnS as a function of the number of ALD cycles. The film thickness deposited by ALD increased linearly with the number of ALD cycles, which represents the characteristics of ALD, including its precise thickness control and reasonable uniformity. The deposition rate of each thin film was defined as the thickness increase per ALD cycle (nm/cycle). In this graph, the slopes obtained by linear regression were considered to be the deposition rate. In the case of ZnS, the deposition rate was 0.069 nm/cycle, which is nearly identical to the values found in the literature [24]. The deposition rate of Al_2O_3 was 0.084 nm/cycle, which is slightly lower than one reported value (0.12 nm/cycle) [25]. The deposition rate of ZnO was 0.125 nm/cycle, which was lower than that of 0.2 nm/cycle, as stated in another study [23]. All the deposition rates, including our results and reported values by other researchers, were less than one monolayer (unit cell length). The reason for smaller value of growth rate by 1 cycle than 1 layer (unit cell length) mainly comes from the difference in molecular size between the precursor molecule ($Al(CH_3)_3$ or H_2O) and the corresponding atom (Al or O) in the final solid film material. Although the partial

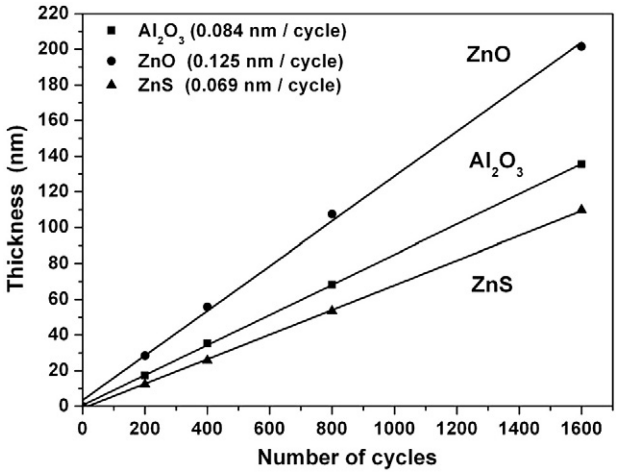

Fig. 1. Film thickness of Al_2O_3, ZnO and ZnS on Si(100) as a function of the number of cycles.

pressure of $Al(CH_3)_3$ is high enough to saturate all the adsorption sites, three bulky methyl groups ($-CH_3$) might inhibit the adsorption of the adsorbate (TMA) in the nearest adsorption sites by steric hindrance and repulsion of bulky ligands. Precursor molecules occupy more than one site due to the larger molecular size compared to the corresponding atom. The lower molecular density of the precursor compared to that of corresponding atom was well-explained in reference [26]. Comparing the present ALD conditions given in Table 1 to previous reports more precisely [27], the lower deposition rates of the Al_2O_3 and ZnO thin films compared to those in earlier studies are probably caused by a higher deposition temperature (300 °C) [27]. Deposition temperature is likely to be the main factor for the lower deposition rate because a higher deposition temperature reduces the adsorption amount of precursors on the substrate. A smaller amount of adsorbed precursor will result in a low deposition rate. In this experimental condition, precursor saturation is ensured due to longer TMA feeding time (0.5 s) compared to other conditions (0.02 s) in a previous report [28].

The physical properties of ZnO were closely related to the ALD process conditions, especially the purge time. Krajewski et al. reported that a low free electron concentration was achieved with a longer purging time (20 s) after H_2O feeding because the longer purging time likely protects the accumulation of the hydroxyl group in the thin film [28]. As the main goal of this study was to investigate the effect of a passivation layer on ZnO, a relatively longer purge time (10 s) was used to obtain high-quality ZnO with minimum the variations of the ZnO itself.

To reveal the effects of changes on various parameters, such as the ZnO thickness, ZnS passivation layer, and Al_2O_3 buffer layer, a series of multi-layers with different thicknesses were designed and prepared by ALD, as shown in Table 2. The total number of ALD cycles for the formation of the ZnO thin film was 800 for a thickness of 120 nm and 1600 for a thickness of 240 nm. These values for ZnS

Table 1
ALD conditions for the formation of the ZnO, ZnS, and Al_2O_3 thin films.

Material	Zn or Al precursor	O or S precursor	Substrate temperature (°C)	Step time (s)			
				(1)* Feeding	(2)# Purging	(3)^ Feeding	(4) Purging
Al_2O_3	TMA ($Al(CH_3)_3$)	H_2O	300	0.5	1.0	1.0	10.0
ZnO	DEZn ($Zn(C_2H_5)_2$)	H_2O	300	0.5	1.0	1.0	10.0
ZnS	DEZn ($Zn(C_2H_5)_2$)	H_2S	300	0.5	1.0	1.0	8.0

*(1) Metal precursor feeding (TMA or DEZn).
#(2) Argon purging.
^(3) Oxygen or sulfur precursor feeding (H_2O or H_2S).

Table 2
Multi-layer structure of the samples prepared by ALD.

Sample number	Multi-layer structure
1	Si/ZnO 120 nm
2	Si/ZnS/ZnO 120 nm/ZnS
3	Si/ZnO 240 nm
4	Si/ZnS/ZnO 240 nm/ZnS
5	Si/Al_2O_3/ZnO 120 nm
6	Si/Al_2O_3/ZnS/ZnO 120 nm/ZnS
7	Si/Al_2O_3/ZnO 240 nm
8	Si/Al_2O_3/ZnS/ZnO 240 nm/ZnS

and Al_2O_3 were fixed at 100 and 200 for thicknesses of 7 nm and 17 nm, respectively. ZnS was used as a passivation layer or a buffer layer with Al_2O_3 as a buffer layer.

Fig. 2 shows XRD patterns of the ZnO single-layer and ZnS/ZnO/ZnS multi-layer thin films on Si (100) and Si(100)/Al_2O_3. Fig. 2(a) shows XRD patterns of the ZnO and ZnS/ZnO/ZnS multi-layer thin films grown on Si (100). ZnO single-layer thin film grown on Si (100) displays sharp peaks corresponding to the hexagonal wurtzite structure. The intensities of these peaks increased as the thickness of the ZnO increased from 120 nm to 240 nm. Among these peaks, a peak at 34° which corresponded to (002), showed a particularly high intensity compared to the other peaks. This indicates that ZnO as formed on Si(100) has a preferred (002) orientation. In the case of the ZnS/ZnO/ZnS multi-layer thin films grown on Si(100), two crystallized thin film materials, ZnO with a hexagonal wurtzite phase and ZnS with a sphalerite (111) or wurtzite (002) phase judging from a peak at 28°, were detected. The ZnS layer had a very broad peak with low intensity due to a thin thickness of 7 nm. The preferred (002) orientation of ZnO in the ZnS/ZnO/ZnS multi-layer was not as strong as that of the ZnO single-layer. Fig. 2 (b) shows ZnO single-layer and ZnS/ZnO/ZnS multi-layer samples on Si(100)/Al_2O_3. The peak corresponding to ZnO (002) decreased when the substrate was changed from Si(100) to Si(100)/Al_2O_3. On the other hand, the intensities of the two other peaks corresponding to (001) and (101) increased with the same substrate change. This indicates that the preferred (002) orientation of ZnO decreased when the substrate was changed from the crystalline surface of Si(100) to the amorphous Al_2O_3 surface of Si(100)/Al_2O_3. For the ZnS/ZnO/ZnS multi-layer sample, a change of the substrate from Si(100) to Si (100)/Al_2O_3 did not result in any significant change in the peak intensity because ZnS was the uppermost layer in the deposition of the ZnO. These XRD patterns imply that the crystalline Si(100) surface enhances the preferred orientation of ZnO (002), whereas the ZnS surface did not improve the preferred orientation of ZnO (002).

Among the samples, the Al_2O_3/ZnS/ZnO/ZnS multi-layer sample on the Si wafer (Si/Al_2O_3/ZnS/ZnO/ZnS) was selected for the TEM analysis to obtain cross-sectional images, as shown in Fig. 3. This sample was chosen because it had the most complex structure among all the prepared samples and because it contained all of the different

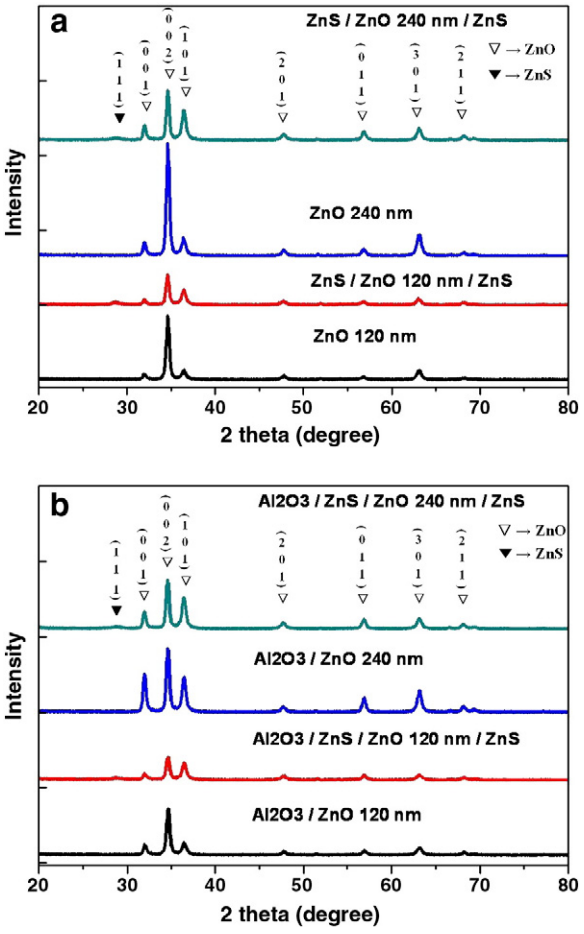

Fig. 2. X-ray diffraction patterns of the ZnO single layer and ZnS/ZnO/ZnS multi-layer according to the ZnO thickness (120 nm and 240 nm) on (a) Si(100) and (b) Si/Al_2O_3.

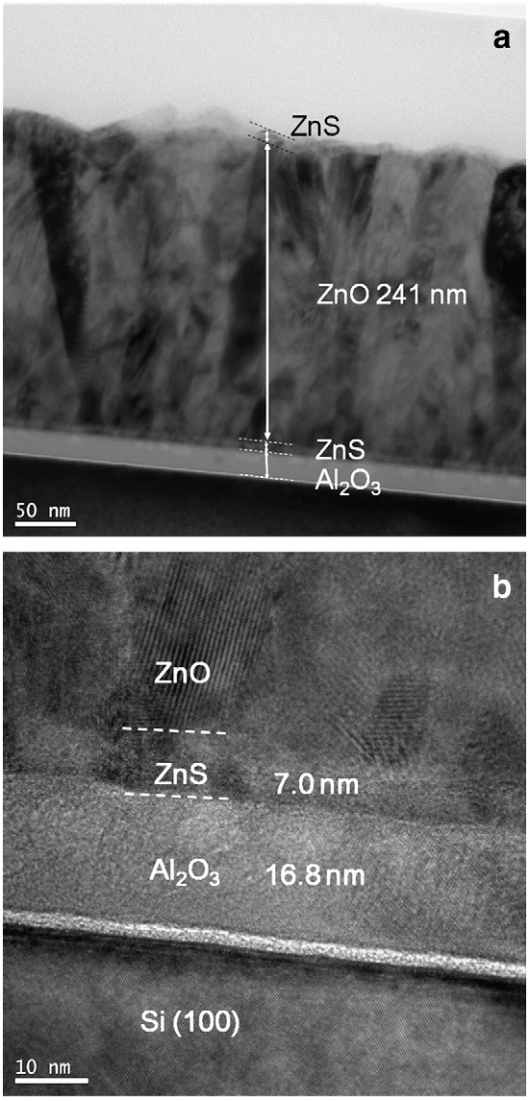

Fig. 3. Cross-sectional transmission electron microscopy images of Si/Al_2O_3/ZnS/ZnO/ZnS multi-layers: (a) entire range (×100,000) and (b) high-resolution (×300,000) image of the interface between the ZnO and Si wafer.

types of thin film used here: ZnO, ZnS, and Al_2O_3. Fig. 3(a) shows that the ZnO and ZnS layers are clearly distinguishable in the ZnS/ZnO/ZnS multi-layer structure. Fig. 3(a) also indicates that the polycrystalline columnar structure is the dominant crystal structure of the ZnO thin film. As shown in Table 3, the thickness of the ZnO measured by TEM was 240 nm, which is slightly different from the thickness (215 nm) calculated according to the deposition rate and ALD cycles. The thickness difference of about 11% may come from the differences in the substrates. When calculating the ZnO thickness, the deposition rate was obtained from a ZnO thin film grown on a Si wafer. However, the ZnO film in the TEM image was actually deposited on the surface of a ZnS buffer layer.

The high-resolution TEM image in Fig. 3(b) displays the interface structure between the ZnO layer and the Si wafer more precisely. As expected, the ZnS layer with a thickness of 7 nm shows a polycrystalline structure while the Al_2O_3 layer with a thickness of 17 nm demonstrates an amorphous domain. The formation of a clearly distinguishable but smooth interface between ZnS and ZnO was also noted. Cross-sectional TEM images of the ZnS/ZnO/ZnS multi-layer on Si/Al_2O_3 confirmed that a ZnS/ZnO/ZnS multi-layer thin film with a clearly distinguishable, smooth interface and polycrystalline domains was formed by ALD.

Based on the XRD and TEM results, the structural properties of the ZnO single layer and the ZnS/ZnO/ZnS multi-layer samples were assessed in terms of their optical properties by photoluminescence (PL) measurement. Fig. 4(a) and (b) shows the PL intensities of the ZnO and ZnS/ZnO/ZnS thin films grown on Si(100) and Si(100)/Al_2O_3. The PL spectra clearly show the appearance of a sharp emission peak in the ultraviolet (UV) region of 380 nm. As shown in Fig. 4(a), the increase of the ZnO thickness enhanced the PL intensity regardless of whether a single-layer or a multi-layer thin film structure was used. Comparing the ZnS/ZnO/ZnS multi-layer and the ZnO single layer, the PL intensity of the ZnS/ZnO/ZnS multi-layer was at least twice that of the ZnO single layer at a given ZnO thin film thickness. Fig. 4(b) displays similar results. The ZnS/ZnO/ZnS multi-layer and the ZnO single layer were formed on Si(100)/Al_2O_3. The PL intensity of the ZnS/ZnO/ZnS multi-layer was much higher than that of the ZnO single layer when the ZnO thickness was equal. This indicates that the presence of the ZnS layer over and under the ZnO thin film increases the PL intensity of the ZnO thin film regardless of the substrate [Si(100) or Si(100)/Al_2O_3]. The enhancement of the ZnO PL intensity in the presence of a ZnS layer is likely to be related to the removal of the surface defects on ZnO by the ZnS deposition process. As shown in Fig. 3, the ZnS/ZnO/ZnS multilayer shows a smooth interface between the ZnO and ZnS thin films. This indicates that the surface defects, especially generated by the absence of O or Zn, during and after the ZnO deposition process may have been cured by the ZnS deposition step. Generally, defects are known to be sites for non-radiative recombination. Thus, reducing the surface defects by ZnS deposition may play a role in the enhancement of the ZnO PL intensity.

To investigate the relationship between defects and PL intensity, ZnO thin films prepared by ALD were annealed in vacuum (less than 1.33 Pa) at 300 °C with different treatment times. Fig. 5 reveals

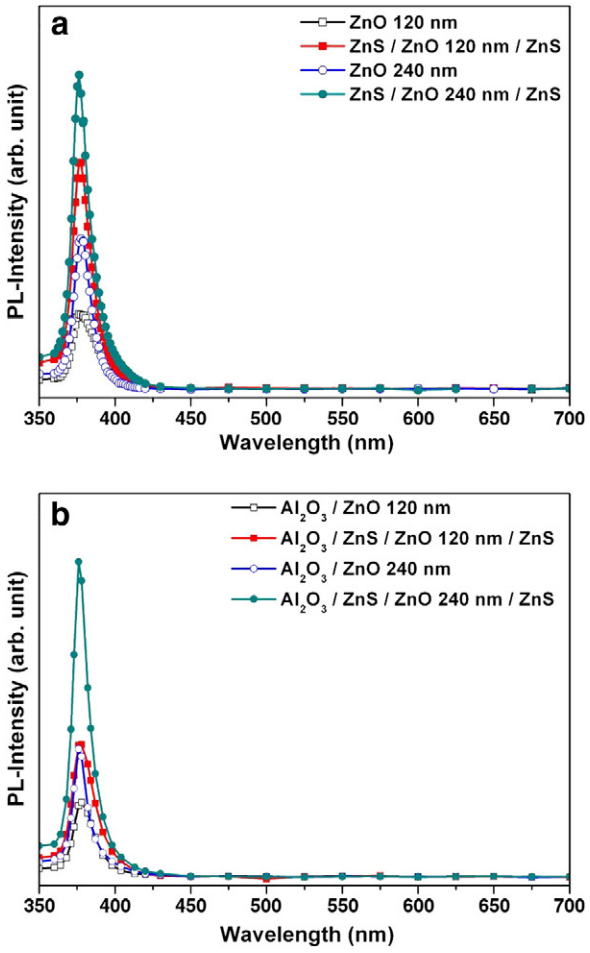

Fig. 4. Photoluminescence spectra of the ZnO single layer and ZnS/ZnO/ZnS multi-layer according to the ZnO thickness (120 nm and 240 nm) on (a) Si(100) and (b) Si/Al_2O_3.

that the PL intensity of the ZnO thin film with the same thickness decreased according to the increase of vacuum treatment time. Vacuum treatment is believed to generate oxygen vacancy defects in ZnO thin film [29,30]. Considering these reports, defects generated by vacuum annealing might induce a decrease of PL intensity. The presence of a ZnS layer under and especially over the ZnO thin film might inhibit

Table 3
Comparison of the thin film thickness between the calculated and measured values.

	Number of ALD cycle	Thin film thickness (nm)	
		Calculated*	TEM^
ZnO	1600	215	241
ZnS	100	7.0	7.0
Al_2O_3	200	17	17

^Measured by TEM.
*Calculated by the deposition rate × the number of ALD cycles.

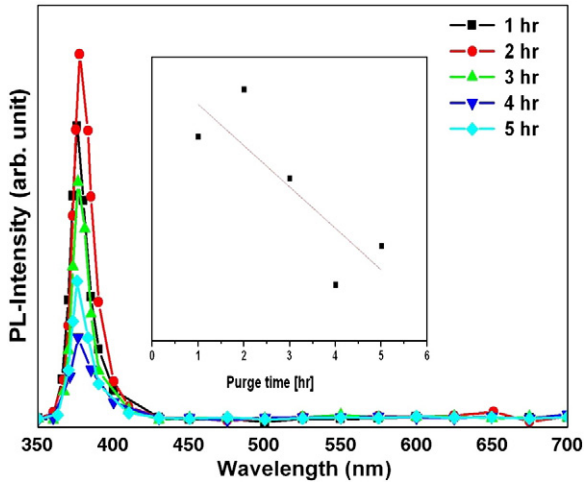

Fig. 5. Change of PL intensity of ZnO thin film by annealing in vacuum at 300 °C according to the vacuum treatment time.

defects generation and cure defects already generated. In particular, over-layer ZnS thin film is expected to play an important role. Ashrafi and co-workers investigated ZnS buffer layer effect on ZnO thin film (GaAs/ZnS/ZnO) [22]. Their paper reported that the buffer layer ZnS in GaAs(001)/ZnS/ZnO enhanced the surface morphology and the crystalline quality of ZnO thin film. However, that paper didn't report an enhancement of PL intensity in ZnO thin film. It indicates that buffer layer is relatively less effective for the enhancement of PL intensity. In this study, the buffer and over layer structure (Si(100)/ZnS/ZnO/ZnS) was prepared to compare that buffer layer only structure (GaAs/ZnS/ZnO). Our result strongly suggests that the upper layer ZnS plays an important role in enhancing ZnO PL intensity. This result indicates that a multi-layer formation of ZnS/ZnO/ZnS will be advantageous in the field of optoelectronic devices. As this multi-layer structure (ZnS/ZnO/ZnS) is effective on an amorphous Al_2O_3 substrate, nanostructure formation using an anodic aluminum oxide template will be a potential application.

4. Conclusions

ZnO single-layer and ZnS/ZnO/ZnS multi-layer films were deposited on Si(100) and Si(100)/Al_2O_3 substrates by ALD. Structural analyses by XRD and TEM showed that these thin films had polycrystalline, well-defined layers with smooth interfaces. Measurement of the PL intensity demonstrated that the ZnS/ZnO/ZnS multi-layer film had twice the PL intensity of the ZnO single-layer at the same ZnO thickness. Introduction of a ZnS thin film layer on the surface of ZnO likely enhances the optical properties of ZnO probably because its formation removes ZnO surface defects.

Acknowledgment

This work was supported by the IT R&D program of MKE/KEIT [10031066, Anisotropic connecting material and component].

References

[1] T. Nakamura, Y. Yamada, T. Kusumori, H. Minoura, H. Muto, Thin Solid Films 411 (2002) 60.
[2] Ü. Özgür, Y.I. Alivov, C. Liu, A. Teke, M.A. Reshchikov, S. Doğan, V. Avrutin, S.-J. Cho, H. Morkoç, J. Appl. Phys. 98 (2005) 041301.
[3] X.-L. Guo, J.-H. Choi, H. Tabata, T. Kawai, Jpn. J. Appl. Phys. 40 (2001) 177.
[4] M. Godlewski, E. Guziewicz, G. Łuka, T. Krajewski, M. Łukasiewicz, Ł. Wachnicki, A. Wachnicka, K. Kopalko, A. Sarem, B. Dalati, Thin Solid Films 518 (2009) 1145.
[5] C.R. Gorla, N.W. Emanetoglu, S. Liang, W.E. Mayo, Y. Lu, J. Appl. Phys. 85 (1999) 2595.
[6] M. Krunks, E. Mellikov, Thin Solid Films 270 (1995) 33.
[7] Y.Y. Villanueva, D.-R. Liu, P.T. Cheng, Thin Solid Films 501 (2006) 366.
[8] D.J. Kang, J.S. Kim, S.W. Jeong, Y. Roh, S.H. Jeong, J.H. Boo, Thin Solid Films 475 (2005) 160.
[9] T.K. Subramanyam, B.S. Naidu, S. Uthanna, Opt. Mater. 13 (1999) 239.
[10] H. Kim, H.-B.-R. Lee, W.-J. Maeng, Thin Solid Films 517 (2009) 2563.
[11] J.D. Ferguson, A.W. Weimer, S.M. George, Thin Solid Films 371 (2000) 95.
[12] S.M. George, A.W. Ott, J.W. Klaus, J. Phys. Chem. 100 (1996) 13121.
[13] J.D. Ferguson, A.W. Weimer, S.M. George, Chem. Mater. 12 (2000) 3472.
[14] B.S. Berland, I.P. Gartland, A.W. Ott, S.M. George, Chem. Mater. 10 (1998) 3941.
[15] M.A. Cameron, I.P. Gartland, J.A. Smith, S.F. Diaz, S.M. George, Langmuir 16 (2000) 7435.
[16] M. Ritala, M. Leskelä, J.-P. Dekker, C. Mutsaers, P.J. Soininen, J. Skarp, Chem. Vap. Deposition. 5 (1999) 7.
[17] J.W. Elam, Z.A. Sechrist, S.M. George, Thin Solid Films 414 (2002) 43.
[18] Z.W. Li, W. Gao, R.J. Reeves, Surf. Coat. Technol. 198 (2005) 319.
[19] J. Lim, C. Lee, Thin Solid Films 515 (2007) 3335.
[20] I.A. Kowalik, E. Guziewicz, K. Kopalko, S. Yatsunenko, A.W. Glodowska, M. Godlewski, P. Dluz˙ewski, E. Łusakowska, W. Paszkowicz, J. Cryst. Growth 311 (2009) 1096.
[21] J. Lim, K. Shin, H.W. Kim, C. Lee, J. Lumin. 109 (2004) 181.
[22] A.A. Ashrafi, A. Ueta, H. Kumano, I. Suemune, J. Cryst. Growth 221 (2000) 435.
[23] S. Lee, Y.H. Im, S.H. Kim, Y.B. Hahn, Superlattices Microstruct. 39 (2006) 24.
[24] Y.S. Kim, S.J. Yun, Appl. Surf. Sci. 229 (2004) 105.
[25] M.D. Groner, F.H. Fabreguette, J.W. Elam, S.M. George, Chem. Mater. 16 (2004) 639.
[26] M. Ylilammi, Thin Solid Films 279 (1996) 124.
[27] Y.-S. Min, C.J. An, S.K. Kim, J. Song, C.S. Hwang, Bull Kor. Chem. Soc. 31 (2010) 2503.
[28] T. Krajewski, E. Guziewicz, M. Godlewski, L. Wachnicki, I.A. Kowalik, A.W. Glodowska, M. Lukasiewicz, K. Kopalko, V. Osinniy, M. Guziewicz, Microelectron. J. 40 (2009) 293.
[29] L. Schmidt-Mende, J.L. MacManus-Driscoll, Mater. Today 10 (2007) 40.
[30] G.W. Tomlins, J.H. Routhbort, T.O. Mason, J. Appl. Phys. 87 (2000) 117.